

General Disclaimer

One or more of the Following Statements may affect this Document

- This document has been reproduced from the best copy furnished by the organizational source. It is being released in the interest of making available as much information as possible.
- This document may contain data, which exceeds the sheet parameters. It was furnished in this condition by the organizational source and is the best copy available.
- This document may contain tone-on-tone or color graphs, charts and/or pictures, which have been reproduced in black and white.
- This document is paginated as submitted by the original source.
- Portions of this document are not fully legible due to the historical nature of some of the material. However, it is the best reproduction available from the original submission.

**NASA TECHNICAL
MEMORANDUM**

NASA TM X-72810

NASA TM X-72810

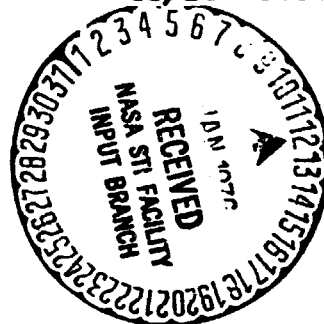
Mossbauer Effect in Dilute Iron Alloys

(NASA-TM-X-72810) MOSSBAUER EFFECT IN
DILUTE IRON ALLOYS (NASA) 35 p HC \$4.00
CSCL 11P

N76-14241

Unclass
06814

G3/26



By Jag J. Singh

This informal documentation medium is used to provide accelerated or special release of technical information to selected users. The contents may not meet NASA formal editing and publication standards, may be revised, or may be incorporated in another publication.

**NATIONAL AERONAUTICS AND SPACE ADMINISTRATION
LANGLEY RESEARCH CENTER, HAMPTON, VIRGINIA 23665**

1. Report No. NASA TM X-72810		2. Government Accession No.		3. Recipient's Catalog No.	
4. Title and Subtitle Mossbauer Effect in Dilute Iron Alloys				5. Report Date December 17, 1975	
				6. Performing Organization Code 1200	
7. Author(s) Jag J. Singh				8. Performing Organization Report No.	
9. Performing Organization Name and Address NASA Langley Research Center Hampton, VA 23665				10. Work Unit No. 505-02-31-02	
				11. Contract or Grant No.	
12. Sponsoring Agency Name and Address National Aeronautics and Space Administration Washington, DC 20546				13. Type of Report and Period Covered Technical Memorandum	
				14. Sponsoring Agency Code	
15. Supplementary Notes The unresolved dilute binary alloy (Fe X) spectra can be analyzed in terms of effective Mossbauer parameters related to the solute concentration.					
16. Abstract The effects of variable concentration, x, of Aluminum, Germanium, and Lanthanum atoms in Iron lattice on various Mossbauer parameters have been studied. Dilute binary alloys of (Fe-Al), (Fe-Ge), and (Fe-Al) containing up to x = 2 at/o of the dilute constituent were prepared in the form of ingots and rolled to a thickness of 0.001". Mossbauer spectra of these targets were then studied in transmission geometry to measure changes in the hyperfine field, peak widths isomer shifts as well as the ratio of the intensities of peaks (1, 6) to the intensities of peaks (2, 5). It has been shown that the concept of effective hyperfine structure field in very dilute alloys provides a useful means of studying the effects of progressively increasing the solute concentration on host lattice properties. An effective hyperfine structure field measurement can be used to infer the impurity/defect distribution changes needed in Fracture Mechanics Studies.					
17. Key Words (Suggested by Author(s)) (STAR category underlined) Metallic Materials, Mossbauer Effect, Iron Alloys, Magnetic Properties, Impurities, Crystal Defects, Crystal Dislocations, Fatigue (Materials), Nondestructive Tests.				18. Distribution Statement: Unclassified - Unlimited Star Category - 26	
19. Security Classif. (of this report) Unclassified		20. Security Classif. (of this page) Unclassified		21. No. of Pages 34	22. Price* \$3.75

LIST OF CONTENTS

	<u>Page</u>
ABSTRACT	1
INTRODUCTION	1
EXPERIMENTAL PROCEDURE	4
EXPERIMENTAL RESULTS AND DISCUSSION	5
CONCLUDING REMARKS	10
REFERENCES	11
APPENDICES	29

MOSSBAUER EFFECT IN DILUTE IRON ALLOYS

Jag J. Singh
NASA Langley Research Center
Hampton, Va.

ABSTRACT

The effects of variable concentration, x , of Aluminum, Germanium, and Lanthanum atoms in Iron lattice on various Mossbauer parameters have been studied. Dilute binary alloys of (Fe-Al), (Fe-Ge), and (Fe-La) containing up to $x = 2$ a/o of the dilute constituent were prepared in the form of ingots and rolled to a thickness of 0.001". Mossbauer spectra of these targets were then studied in transmission geometry to measure changes in the hyperfine field, peak widths and isomer shifts as well as the ratio of the intensities of peaks (1, 6) to the intensities of peaks (2, 5). It has been shown that the concept of effective hyperfine structure field in very dilute alloys provides a useful means of studying the effects of progressively increasing the solute concentration on host lattice properties. An effective hyperfine structure field measurement can be used to infer the impurity/defect distribution changes needed in Fracture Mechanics Studies.

INTRODUCTION

Solute atoms in dilute iron alloys have an important bearing on their microscopic and macroscopic properties. In the simplest case, the non-magnetic solute atoms would randomly enter the host lattice and dilute the effective atomic moment of the host atoms. However, some recent accurate studies of the ferromagnetic properties of various binary alloys have revealed a more complicated behavior even for nonmagnetic metal impurities. Generally, the impurity atoms participate in the conduction process thereby affecting the charge (and spin) density at the host lattice sites. These changes in the electronic charge density affect the electrostatic interaction with the nucleus, leading to changes in the position of nuclear energy levels. Besides the local hyperfine interactions the presence of the impurity atoms also affects the elastic properties of the lattice cells and thus the alloy physical properties - such as yield strength and the fatigue behavior. Consequently, the information about the impurity atom distribution is of great interest to the physicist as well as the physical metallurgist. It is the purpose of this report to discuss the use of Mossbauer effect in inferring solute atom distribution in dilute iron alloys as a function of the solute concentration.

The subject of this paper is an Fe⁵⁷ Mossbauer effect study of iron-rich alloys Fe X, where X is either Al, Ge, or La and its concentration ranges from 0 → 2 a/o. The observed Mossbauer spectra at all concentration

levels appeared to be normal Lorentzian 6-peak patterns expected in pure iron foils and are analyzed as such in order to determine the hyperfine structure (hfs) peak positions and the line widths. (See appendix A for further discussion of unresolved spectra.) From the observed peak positions, the values of effective hfs field and the isomer shift are calculated. The hfs field values thus deduced are compared with the effective internal field values calculated on the basis of local magnetic fields in random binary solid solution, as follows:

$$H_{(eff)} = \frac{\sum_i \left[P_{(n, m)} \right]_i \left[H_{(n, m)} \right]_i}{\sum_i \left[P_{(n, m)} \right]_i} \quad (1)$$

where $\left[P_{(n, m)} \right]_i$ = probability of finding the ith combination of n impurity atoms in 1 nn and m impurity atoms in the 2 nn shells.

$$n, m < (n + m) < 3^{(*)}$$

$\left[H_{(n, m)} \right]_i$ = hfs field corresponding to the ith impurity atom distribution

$$= H_{Fe} \left[(1 + an + bm) (1 + kc) \right]_i \quad (2)$$

n = number of impurity atoms in 1 nn

m = number of impurity atoms in 2 nn

c = fractional concentration of impurity atoms

a, b, k = constants to be determined by least squares fit of the experimental hfs field distribution to equation (1).

(*) For impurity concentration < 2.0 a/o, it is unlikely that there will be more than three impurity atoms in the 1 nn and 2 nn shells at any one time. (See appendix B for detailed calculations. Also, see discussion on pages 6 and 7.)

The effective field concept was used for the following reasons:

1. It is difficult to resolve close-lying, low intensity, satellite sextets from the dominant sextet because of large natural width of Fe^{57} hyperfine structure (hfs) peaks.
2. Micro-environmental fluctuations in disordered dilute alloys smear out the anticipated satellite structure - particularly at the solute concentration levels of $< 2 \text{ a/o}$.
3. Statistical fluctuations in the experimental data points make it very difficult to resolve the composite spectral lines into a unique set of constituent lines.
4. The alloys show a progressive approach towards randomness of Fe atom spin orientation as a function of the solute concentration. This trend makes it difficult to obtain "true" calculated spectrum for variable solute concentrations.
5. In fatigue damage studies, an estimate of the relative probabilities of various types of atomic environments is not possible because detailed knowledge about the impurity/defect concentration and location is not available. Under such circumstances, the concept of H_{eff} might be more useful since it is dependent only on the location of the experimental centroid of the component lines.

Rigorously, one should obtain the calculated spectrum by summing the spectra for iron atoms with (n, m) impurity neighbors assuming for each type of iron atom an internal field given by $H(n, m)$ and a contribution to the total spectrum proportional to the probability, $P(n, m)$. This calculated spectrum should then be compared with the experimental spectrum in order to test the validity of the calculational model.

It should be mentioned that H_{eff} is rather insensitive to the magnetism model used (i.e., whether localized or diffused band type) as long as one obtains a good single line fit to the experimental data. H_{eff} depends simply on the centroid of the lines of the component spectra and the solutions of different models adjust their values to give essentially the same value for the centroid.

The isomer shift in the alloys is expected to vary with the solute concentration due to changes in the electron density at the nucleus. If there is a change, $\Delta e|\psi_s(0)|^2$, in total charge density at the iron nucleus in an alloy compared with that in the pure iron, the isomer shift change, $\Delta(\text{I.S.})$, can be written as follows:⁽¹⁾

$$\Delta(\text{I.S.}) = 2/5 \pi Z e^2 \left(R_{\text{ex}}^2 - R_{\text{gd}}^2 \right) \Delta |\psi_s(o)|^2 \quad (3)$$

$$= - 7 \times 10^{-26} \Delta |\psi_s(o)|^2 \frac{\text{mm}}{\text{sec}} \quad (4)$$

(using reported values of R_{ex} and R_{gd}).⁽²⁾

Clearly, a reduction in $|\psi_s(o)|^2$ implies a shift in the isomer shift in the positive direction and vice versa. The experimentally observed isomer shift changes as a function of the impurity concentration should thus provide information on $\Delta |\psi_s(o)|^2$ and, hence, the hyperfine field.

A hyperfine field spread resulting from local fluctuations of composition throughout the alloy is expected to be accompanied by the broadening of the line widths.⁽³⁾ When the impurity atoms are nonmagnetic, they provide a rather large local magnetic disturbance resulting in non-negligible line broadening. The line broadening is expected to be much less if the impurity atoms have a large magnetic moment of their own.

Specific results for the three alloy series are discussed in the following pages.

EXPERIMENTAL PROCEDURE

The Mossbauer absorption spectra of Fe^{57} in alloys of iron with two nonmagnetic elements (Al and Ge) and one transition metal (La) have been measured. The alloys were made by induction melting of the mixture of the two components in an argon atmosphere in an alumina crucible. The solute concentration was varied from 0 a/o to 2.0 a/o in steps of 0.5 a/o. The spectroscopic analyses of the various alloy constituents are summarized in Table I below.

Table I.- Summary of the Analyses of Alloy Constituents

Iron 99.95% Purity	Aluminum 99.999% Purity	Lanthanum 99.85% Purity	Germanium Highest Available Purity
Iron - Major	Al - Major	La - Major	It was supplied with no "nines" designation for the purity. But it was first reduction material with a resistivity of > 5 ohm-centimeter
Mn - 0.028%	Si - 5 ppm	Al - 0.04%	
S - 0.025%	Fe - 5 ppm	Si - 0.04%	
C - 0.015%	Mg - 2 ppm	Ca - 0.04%	
P - 0.005%	Cu - 1 ppm	Fe - 0.02%	
Si - 0.003%	Ca - 0.5 ppm	Mg - 0.01%	
	Mn - 0.1 ppm	Y - 0.001%	

The alloy specimen were cold rolled into foils 0.001" thick and cut into 1" x 1" pieces for use as absorbers. A 25 mc Co⁵⁷(Pt) source provided the 14.4 keV Mossbauer radiation. A conventional electromagnetic drive system moved the source at constant acceleration. The velocity calibration was performed using the known⁽⁴⁾ magnetic hyperfine splitting of Fe⁵⁷ in iron. The velocity versus count rate spectrum was recorded using a 1024 channel multichannel analyzer in the time mode of operation. These spectra were analyzed using a computer program described elsewhere.⁽⁵⁾ Figure 1 shows a schematic diagram of the experimental system used in this study.

EXPERIMENTAL RESULTS AND DISCUSSION

For each alloy system, the following parameters were measured as a function of the solute concentration.

- I.S. - Isomer shift of the spectrum
- $\langle \Gamma_{1,6} \rangle$ - Average line width for peaks 1 and 6 in the spectrum
- $\langle G_0 \rangle$ - Average hyperfine splitting for the ground state in Fe⁵⁷ in the alloy
- $\langle G_1 \rangle$ - Hyperfine splitting for the 14.4 keV state in Fe⁵⁷ in the alloy
- M_2 - Ratio of the sum of the areas under lines 1 and 6 to the sum of the areas under lines 2 and 5 in the spectrum.

There appeared to be no quadrupole shift in any of the alloys studied.

The results of the three alloy series are summarized in Tables II - IV.

(Fe-Al) System

Figure 2 shows typical (Fe-Al) alloy Mossbauer spectra for three different aluminum concentrations. It is seen that there are no evident shoulders to the peaks and the fit between the experimental data and the computed curve based on the concept of an effective hfs field is equally good at these different concentrations. (See appendix A for further discussion.)

As seen from the data in Table II, the isomer shift decreases, the line width for the outer peaks increases, the effective hfs field at the Fe^{57} nucleus decreases and the value of M_2 increases in linear proportion to the increasing solute concentration up to 2.0 a/o. The decrease in the isomer shift (i.e., becoming more positive with respect to pure iron) indicates a reduction in the electron density at the nucleus. Such a decrease in the charge density is expected to be accompanied by a corresponding spin density decrease resulting in reduced hfs field, as observed. The line broadening with increasing solute concentration is partially the result of local fluctuations in composition causing a spread in the hfs field values. It also arises from the method of analysis as discussed in appendix A. The increase in M_2 with increasing solute concentration indicates increasing resistance to iron atom spin orientation in Fe-Al alloys during cold rolling.

Figure 3 shows the variation of various parameters as a function of aluminum concentration.

For Al concentration up to 2 a/o, the iron lattice retains its bcc structure. The aluminum atoms enter the iron lattice substitutionally in the various near neighbor shells according to the probabilities given below. (*)

$$P_{(n, m)} = P_n P_m$$

$$= \left[\frac{8! c^n (1-c)^{8-n}}{(8-n)! n!} \right] \left[\frac{6! c^m (1-c)^{6-m}}{(6-m)! m!} \right] \quad (5)$$

when c is the solute concentration.

(*) See appendix B for further details.

The effect of the presence of impurity atoms in the inner shells of iron lattice on the hfs field at the iron nucleus can be expressed as follows: (6)

$$H_{(n,m)} = H_{Fe} (1 + an + bm) (1 + kc) \quad (6)$$

(same as equation (2))

Considering all possible combinations of n and m , one may write the following approximate expression for the effective hfs field: (*)

$$H_{(eff)} = \frac{\sum_i [P_i H(n, m)]_i}{\sum_i P_i} \quad (1)$$

$$= H_{Fe} (1 + a\alpha + b\beta) (1 + kc) \quad (7)$$

where α and β are the weighted values for the impurity atoms in the 1 nn and 2 nn shells, respectively. α and β are functions of the concentration, c . It should be emphasized that the concept of weighted values for impurity occupancy in the inner shells has been used only because the relative probabilities for 1 nn and 2 nn occupancies at concentrations up to 2 a/o are low [(0, 0): (1, 0): (0, 1): 1.00 : 0.16 : 0.12 at 2.0 a/o] and the natural width for Fe⁵⁷ is large (i.e., $\Delta H_{eff} \approx \Gamma$). The effective internal field concept has no general first principle basis. (**)

The calculated values of $H_{(eff)}$ for various concentration values are summarized in Table V.

(*) The effects of 1 nn and 2 nn impurity atoms are expected to be more important than the more distant atoms. We have therefore confined our consideration to the two innermost nn shells. The concentration dependent term $(1 + kc)$ may contain unresolved effects of more distant neighbors. (See appendix B for further details.)

(**) It should be mentioned that the values of H_{eff} are quite independent of the analysis model (i.e., whether localized or diffused band type) for dilute alloy systems.

Table V.- Summary of $H_{(eff)}$ Values for Various Impurity Concentration Levels

Impurity Concentration (in units of atomic fraction)	$H_{(eff)}$ (in units of H_{Fe})
0.0	1.0000
0.005	$(1 + 0.04a + 0.03b) (1 + 0.005k)$
0.010	$(1 + 0.08a + 0.06b) (1 + 0.010k)$
0.015	$(1 + 0.12a + 0.09b) (1 + 0.015k)$
0.020	$(1 + 0.16a + 0.12b) (1 + 0.020k)$

Comparing the calculated hfs field values with the experimentally observed field values, the following values for a, b, and k have been obtained:

$$\begin{aligned} a &= \begin{pmatrix} -0.046 \\ 0 \\ 0 \end{pmatrix} \quad \text{or} \quad \begin{pmatrix} -0.081 \\ -0.046 \\ +0.53 \end{pmatrix} \\ b &= \begin{pmatrix} 0 \\ 0 \\ 0 \end{pmatrix} \\ k &= \begin{pmatrix} 0 \\ 0 \\ 0 \end{pmatrix} \end{aligned}$$

Figure 4 shows observed $\left[\frac{H_{(eff)}}{H_{Fe}} \right]$ ratio as a function of aluminum concentration. Data from references 6 and 7 are also shown in this figure.

(Fe-Ge) System

Figure 5 shows typical (Fe-Ge) alloy Mossbauer spectra for three different germanium concentrations. There are no evident shoulders to the peaks and the fit between the experimental data points and the computed curve based on the concept of an effective hfs field is equally good at these different concentrations. (See appendix A for further discussion.)

Figure 6 shows the variation of various Mossbauer parameters as a function of germanium concentration. Figure 7 shows the variation of $(H_{(eff)}/H_{Fe})$ as a function of germanium concentration. The calculated values of the constants in equation (7) are as follows:

$$\begin{aligned} a &= -0.083 \\ b &= \begin{pmatrix} 0 \\ 0 \end{pmatrix} \quad \text{or} \quad \begin{pmatrix} -0.073 \\ -0.020 \end{pmatrix} \\ k &= 0 \quad \quad \quad +0.060 \end{aligned}$$

The (Fe-Ge) data should be compared with the data for (Fe-Si) and (Fe-Sn) alloys (taken from refs. 6 and 7), also shown in figure 7. The electronic configuration in the Ge atom ($4s^2 4p^2$) is equivalent to that in Si ($3s^2 3p^2$) and Sn ($5s^2 5p^2$) atoms and, consequently, Ge is expected to have similar effects on hfs fields at Fe^{57} nuclei in (Fe-Ge) alloy.

The Ge impurity atoms appear to offer greater resistance to iron atom spin orientation during rolling than the Al atoms with the net results that the iron atom spins are oriented almost randomly in 2 a/o (Fe-Ge) alloys.

(Fe-La) System

Figure 8 shows the variation of various Mossbauer parameters as a function of lanthanum concentration in (Fe-La) alloys. Notice that the effect of La on the various iron Mossbauer parameters is much less marked than that of Al or Ge atoms. It may be the result of similarity of the host and the impurity atom electronic configuration ($3d^6 4s^2$ for Fe and

$5d^1 6s^2$ for La). Figure 9 shows a variation of $\frac{H_{\text{eff}}}{H_{\text{Fe}}}$ as a function of

lanthanum concentration. The calculated values of the constants in equation (7) are as follows:

$$a = -0.015$$

$$b = 0$$

$$k = 0$$

In the preceding discussion, it has been shown that the very dilute binary alloys can be approximated by a weighted inner shell impurity atom occupancy, leading to an "effective" hfs field in the alloy. This field can be measured easily, providing an indirect measure of impurity atom distribution in the dilute alloys. Such information is of considerable interest in fatigue damage studies in metals and metallic alloys where impurities - usually in very low concentration in solid solution - concentrate in the region of high stress, resulting in crack nucleation there. Periodic hfs field determinations can provide a useful indication of the impurity population buildup in the stress concentration region of the experimental specimen.

CONCLUDING REMARKS

The effects of low concentration (≤ 2 a/o) solute atoms in iron-rich alloys have been measured using the Mossbauer technique. It has been shown that the concept of "effective" hyperfine structure field in very dilute alloys provides a useful means for studying the effects of progressively increasing solute concentration on host lattice properties. An "effective" hyperfine structure field measurement can be used to infer the impurity/defect distribution changes needed in Fracture Mechanics Studies.

As might be expected, the electronic configuration of the solute atom is the critical factor in determining its effects on the host atom charge/spin density (and hence the hfs field).

REFERENCES

1. G. K. Wertheim, Mossbauer Effect: Principles and Applications.
(Published by Academic Press, New York, 1964.)
2. (a) S. DeBenedetti, G. Lang, and R. Ingalls: Phys. Rev. Let., 6,
60, 1961.
(b) L. R. Walker, G. K. Wertheim, and V. Jaccarino: Phys. Rev. Let.,
6, 98, 1961.
3. C. E. Johnson, M. S. Ridout, and T. E. Cranshaw: Proc. Phys. Soc.,
81, 1079, 1963.
4. (a) S. S. Hanna, J. Heberle, G. J. Perlow, R. S. Preston, and
D. H. Vincent: Phys. Rev. Let., 4, 513, 1960.
(b) R. S. Preston, S. S. Hanna, and J. Heberle: Phys. Rev., 128,
2207, 1962.
5. L. M. Howser, J. J. Singh, and R. E. Smith, Jr.: NASA TM X-2522, 1972.
6. G. K. Wertheim, V. Jaccarino, J. H. Wernick, and D. N. E. Buchanan:
Phys. Rev. Let., 12, 24, 1964.
7. M. B. Stearns: Phys. Rev., 129, 1136, 1963; Phys. Rev., 147, 439, 1965.
8. G. Czjzek and W. G. Berger: Phys. Rev., 1(B), 957, 1970.

TABLE II
MOSSBAUER PARAMETERS FOR (Fe-Al) ALLOYS FOR
VARIABLE AL. CONCENTRATION

ALUMINUM CONC. A/O	I.S., MM/SEC	$\langle \Gamma_{1,6} \rangle$ MM/SEC	$\langle G_0 \rangle$ MM/SEC	$\langle G_1 \rangle$ MM/SEC	$M_2 = \left(\frac{A_1 + A_2}{A_2 + A_5} \right)$
0.0	- 0.3849 ± 0.0025	0.2927 ± 0.0050	3.9053 ± 0.0154	2.2457 ± 0.0154	0.9517 ± 0.0010
0.5	- 0.3836 ± 0.0026	0.3113 ± 0.0037	3.9005 ± 0.0137	2.2429 ± 0.0137	1.0160 ± 0.0030
1.0	- 0.3831 ± 0.0032	0.3611 ± 0.0045	3.8986 ± 0.0048	2.2239 ± 0.0048	1.0569 ± 0.0080
1.5	- 0.3813 ± 0.0033	0.3756 ± 0.0048	3.8825 ± 0.0036	2.2338 ± 0.0036	1.0653 ± 0.0060
2.0	- 0.3800 ± 0.0037	0.4068 ± 0.0053	3.8729 ± 0.0066	2.2278 ± 0.0066	1.2409 ± 0.0100

TABLE III
MOSSBAUER PARAMETERS FOR (Fe-Ge) ALLOYS FOR

VARIABLE GE. CONCENTRATION

GE CONC. A/O	I.S., MM/SEC	$\langle \Gamma_{1,6} \rangle$ MM/SEC	$\langle G_0 \rangle$ MM/SEC	$\langle G_1 \rangle$ MM/SEC	$M_2 = \frac{A_1 + A_6}{A_2 + A_5}$
0	- 0.3848 ± 0.0025	0.2942 ± 0.0036	3.9075 ± 0.0154	2.2445 ± 0.0154	0.9474 ± 0.0010
0.5	- 0.3815 ± 0.0025	0.3039 ± 0.0036	3.8898 ± 0.0101	2.2418 ± 0.0101	1.0800 ± 0.0020
1.0	- 0.3778 ± 0.0030	0.3557 ± 0.0042	3.8803 ± 0.0077	2.2307 ± 0.0077	1.2350 ± 0.0060
1.5	- 0.3757 ± 0.0040	0.3933 ± 0.0058	3.8694 ± 0.0042	2.2137 ± 0.0042	1.1166 ± 0.0090
2.0	- 0.3695 ± 0.0049	0.5721 ± 0.0282	3.8656 ± 0.0060	2.2178 ± 0.0060	1.4173 ± 0.0130

TABLE IV
MOSSBAUER PARAMETERS FOR (Fe-La) ALLOYS FOR

VARIABLE LA. CONCENTRATION

LA CONC. A/O	I.S., MM/SEC	$\langle \Gamma_{1,6} \rangle$ MM/SEC	$\langle G_0 \rangle$ MM/SEC	$\langle G_1 \rangle$ MM/SEC	$M_2 = \frac{A_1 + A_6}{A_2 + A_5}$
0	- 0.3837 \pm 0.0026	0.3006 \pm 0.0038	3.8974 \pm 0.0143	2.2377 \pm 0.0143	0.9240 \pm 0.0020
0.5	- 0.3854 \pm 0.0030	0.3216 \pm 0.0042	3.8879 \pm 0.0101	2.2350 \pm 0.0101	0.9462 \pm 0.0020
1.0	- 0.3827 \pm 0.0025	0.2933 \pm 0.0035	3.8926 \pm 0.0107	2.2406 0.0107	0.9664 \pm 0.0030
1.5	- 0.3809 \pm 0.0026	0.3137 \pm 0.0038	3.8912 \pm 0.0060	2.2267 \pm 0.0060	0.9657 \pm 0.0020
2.0	- 0.3806 \pm 0.0025	0.2937 \pm 0.0036	3.8798 \pm 0.0188	2.2443 \pm 0.0188	0.9172 \pm 0.0020

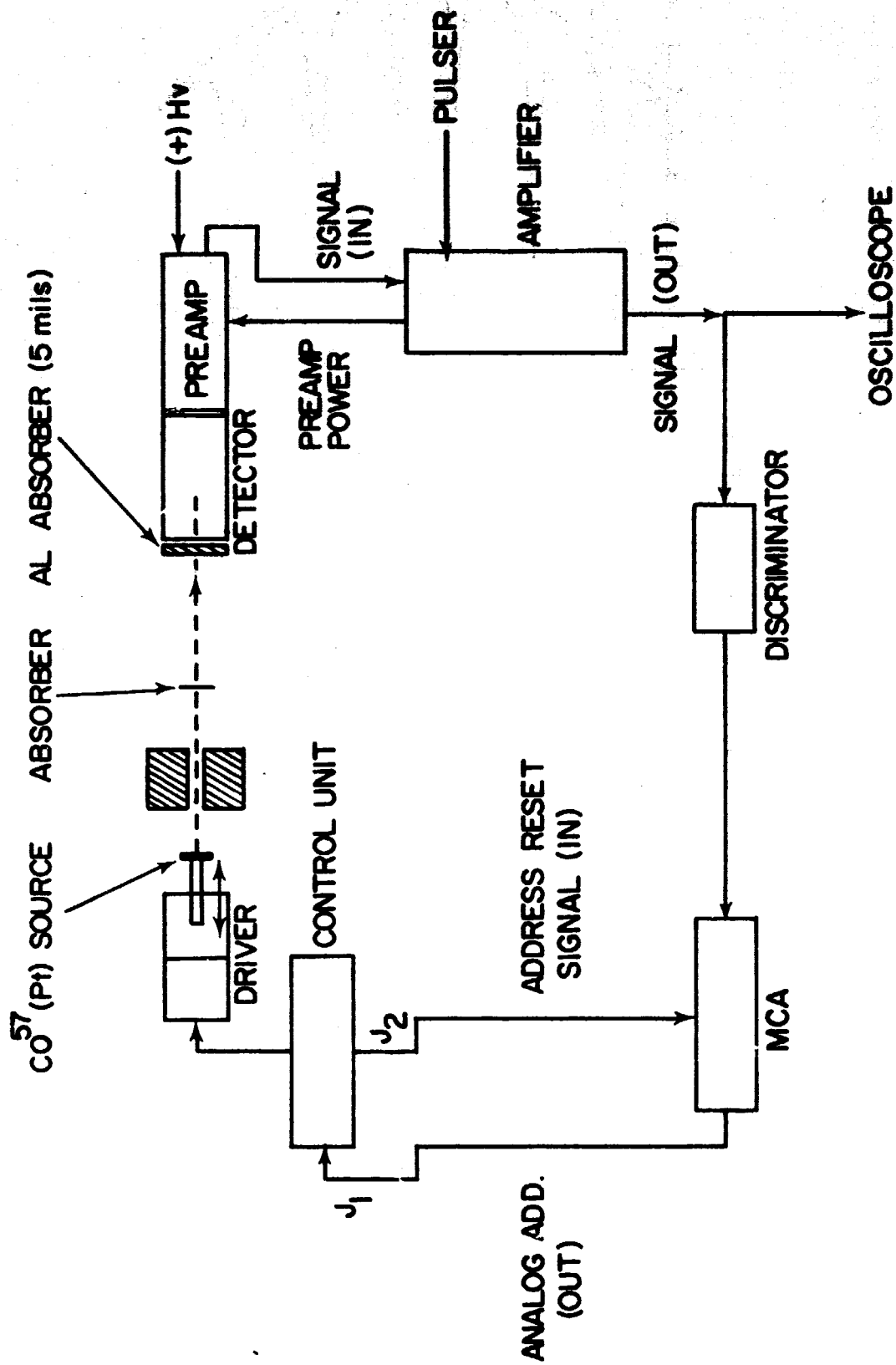


Figure - 1. Schematic diagram of the experimental set-up for measuring Mossbauer spectra.

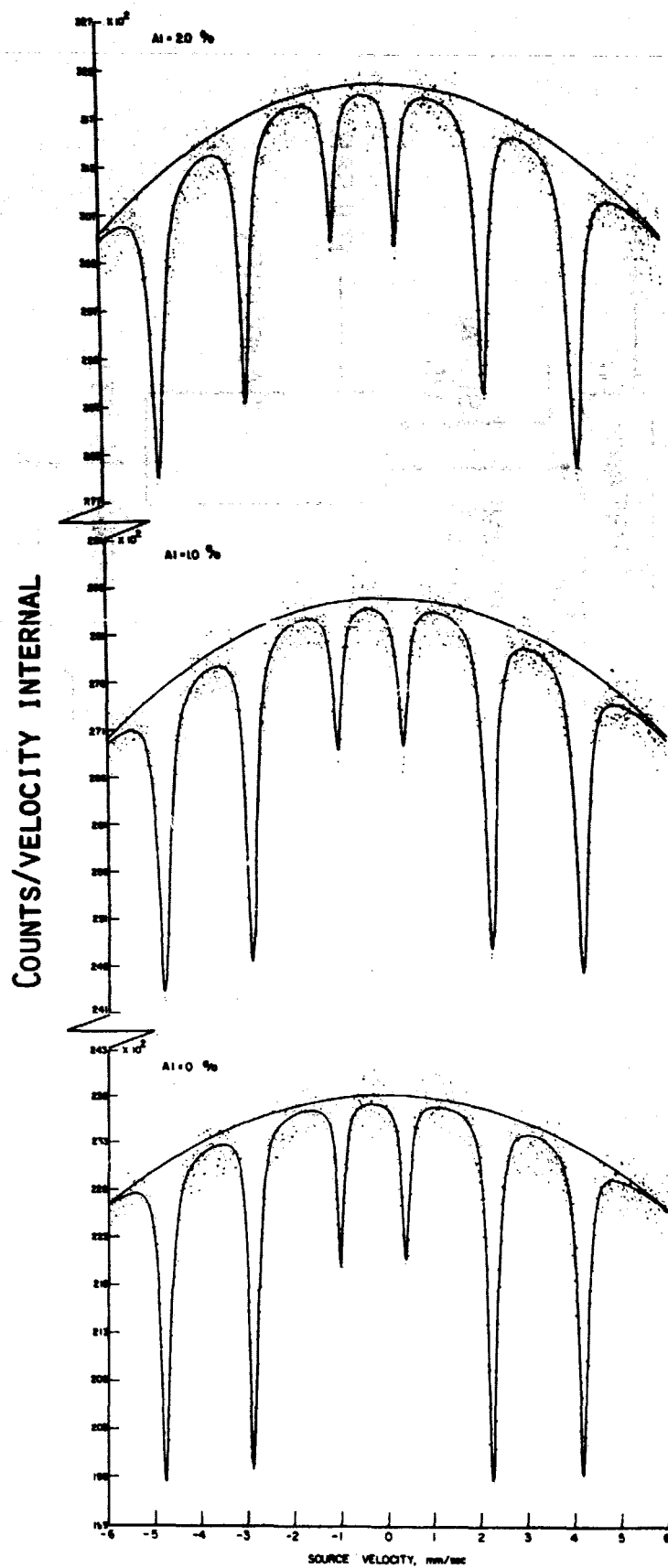


FIGURE-2. EFFECT OF INCREASING AL CONCENTRATION IN MOSSBAUER SPECTRA IN (Fe-AL) ALLOYS

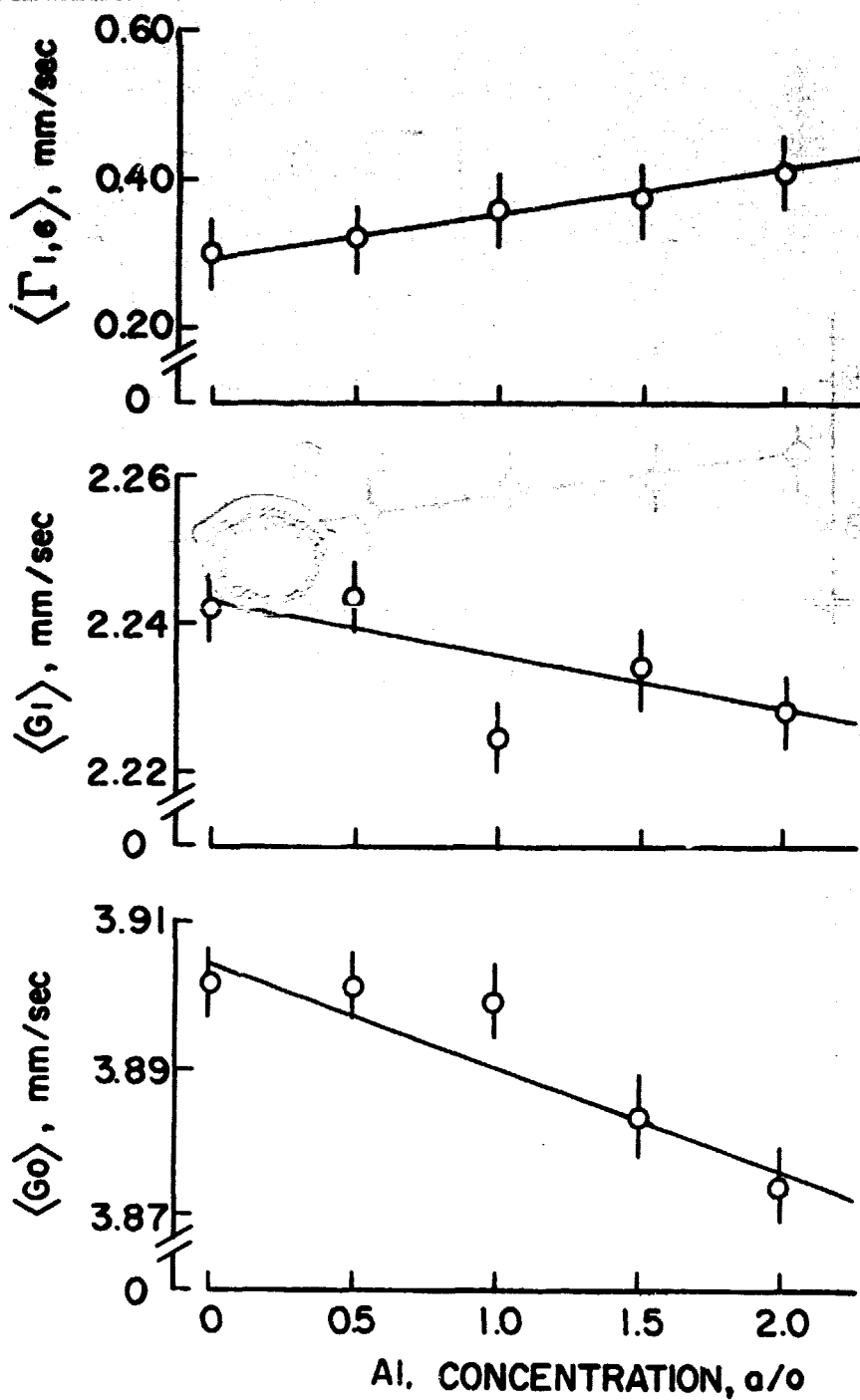


FIGURE-3(a). MOSSBAUER PARAMETER VARIATION IN (Fe-AL) ALLOY AS A FUNCTION OF AL CONCENTRATION

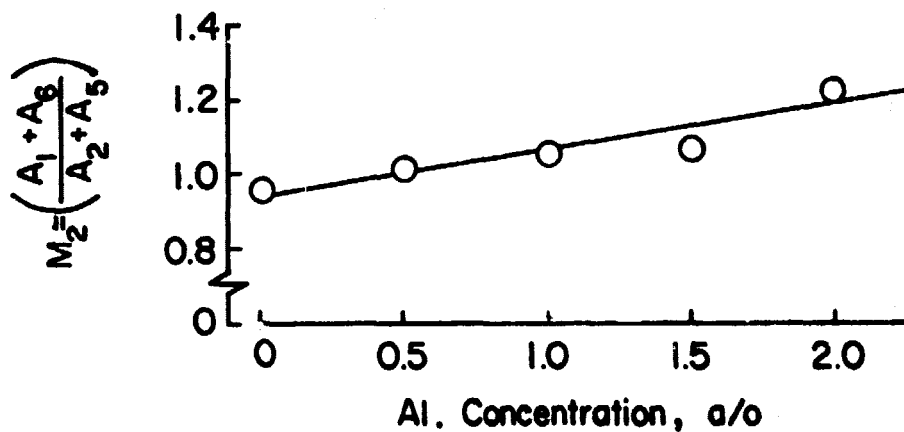
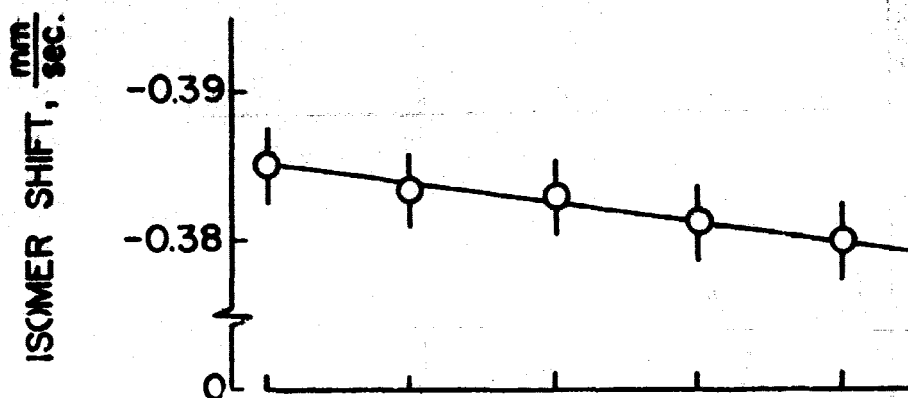


Figure-3(b). Mossbauer parameter variation in (Fe-Al) alloy as a function of Al Concentration.

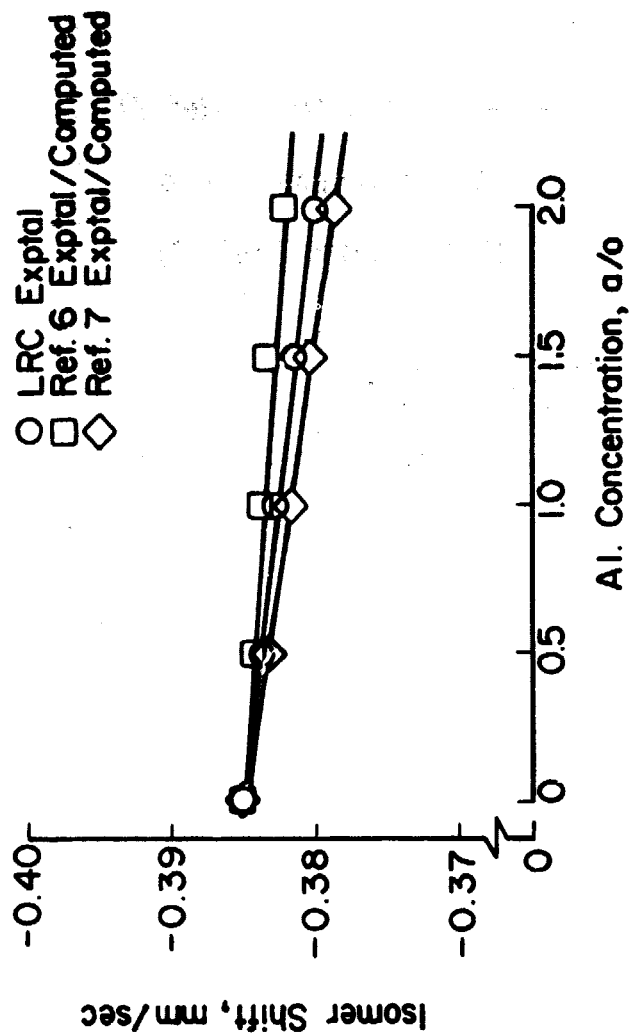


Figure -3(c) Isomer Shift variation in (Fe-Al) alloy as a function of Al Concentration. Also shown are corresponding data from Refs 6 and 7.

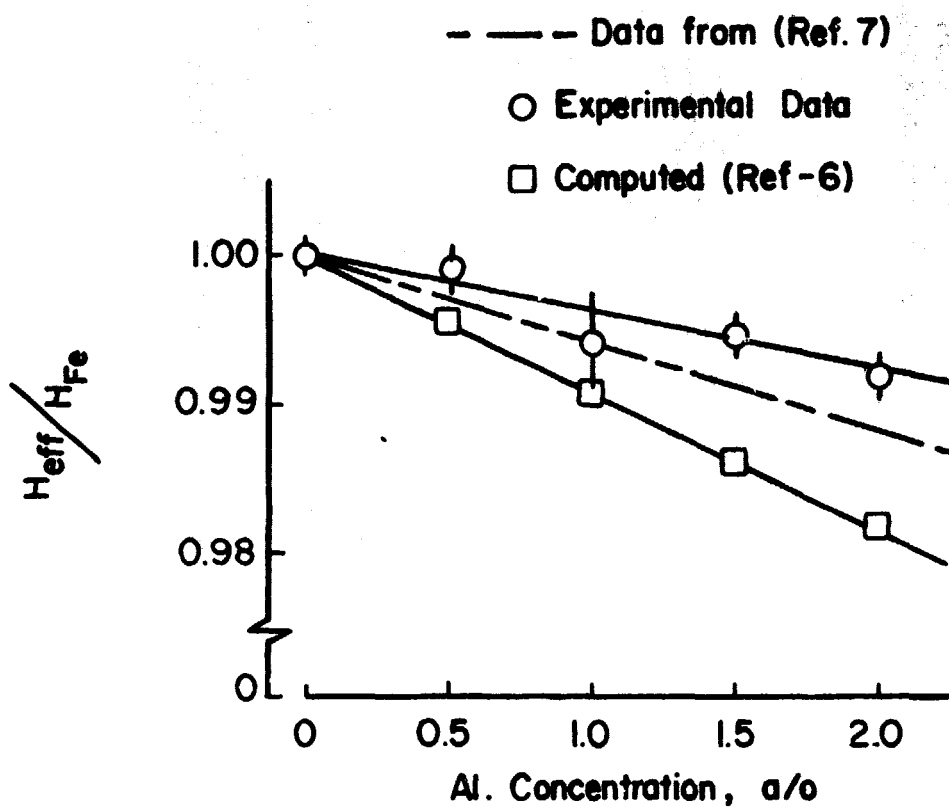


Figure-4. Reduction in hfs field as a function of Al Concentration in (Fe-Al) alloy.

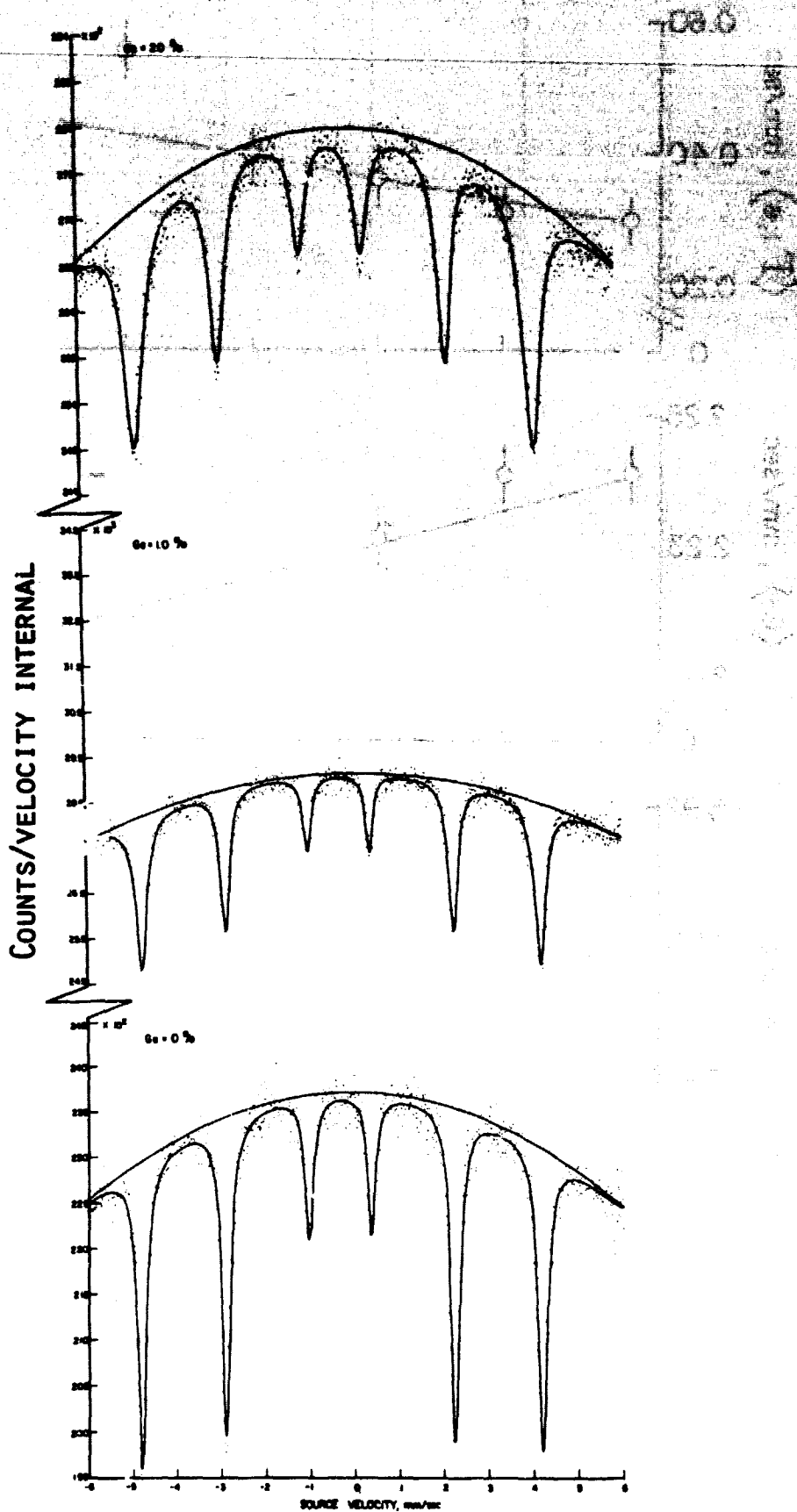


FIGURE-5. EFFECT OF INCREASING GE CONCENTRATION ON MOSSBAUER SPECTRA IN (Fe-Ge) ALLOYS.

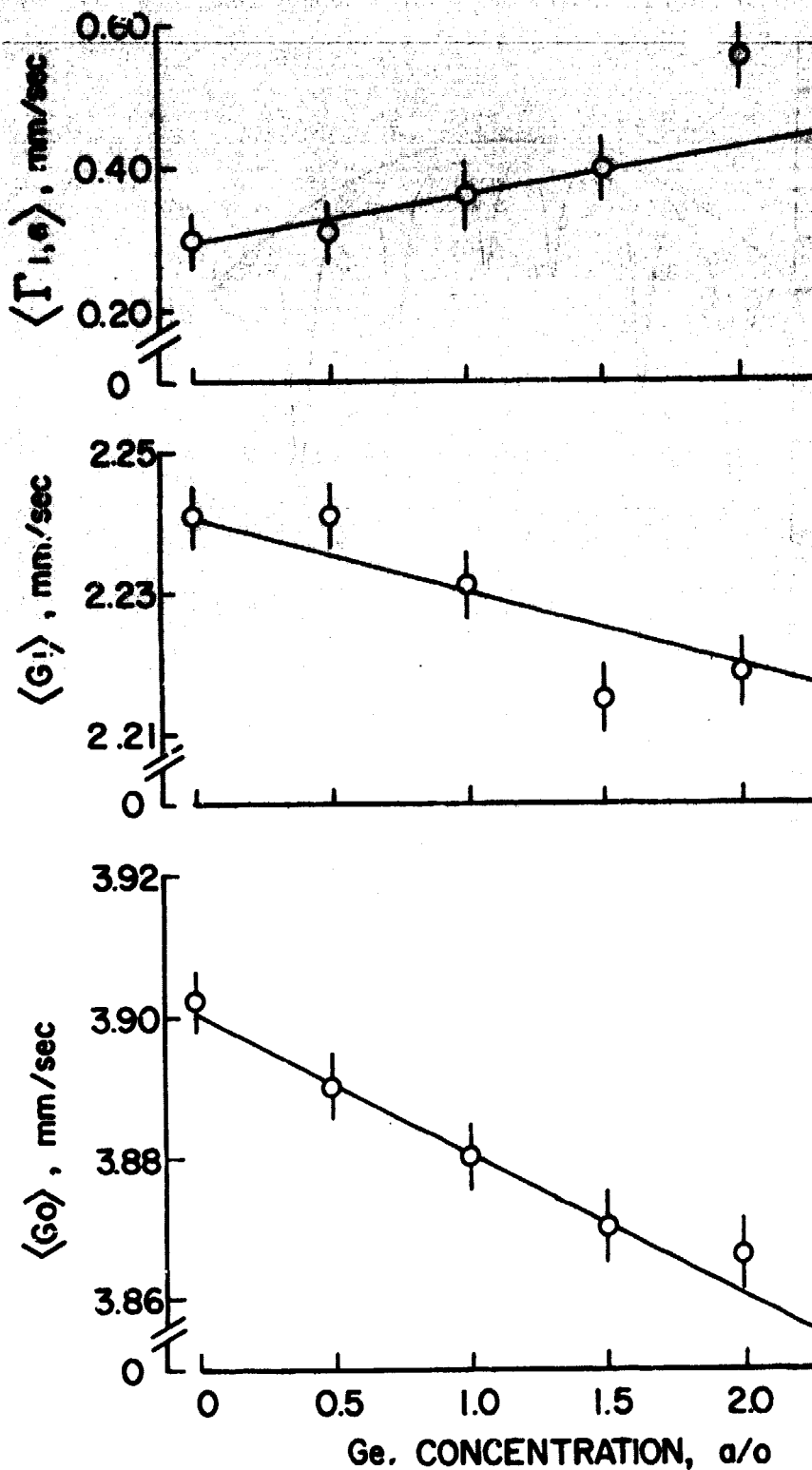


FIGURE-6(a). MOSSBAUER PARAMETER VARIATION IN (Fe-Ge) ALLOY AS A FUNCTION OF GE CONCENTRATION.

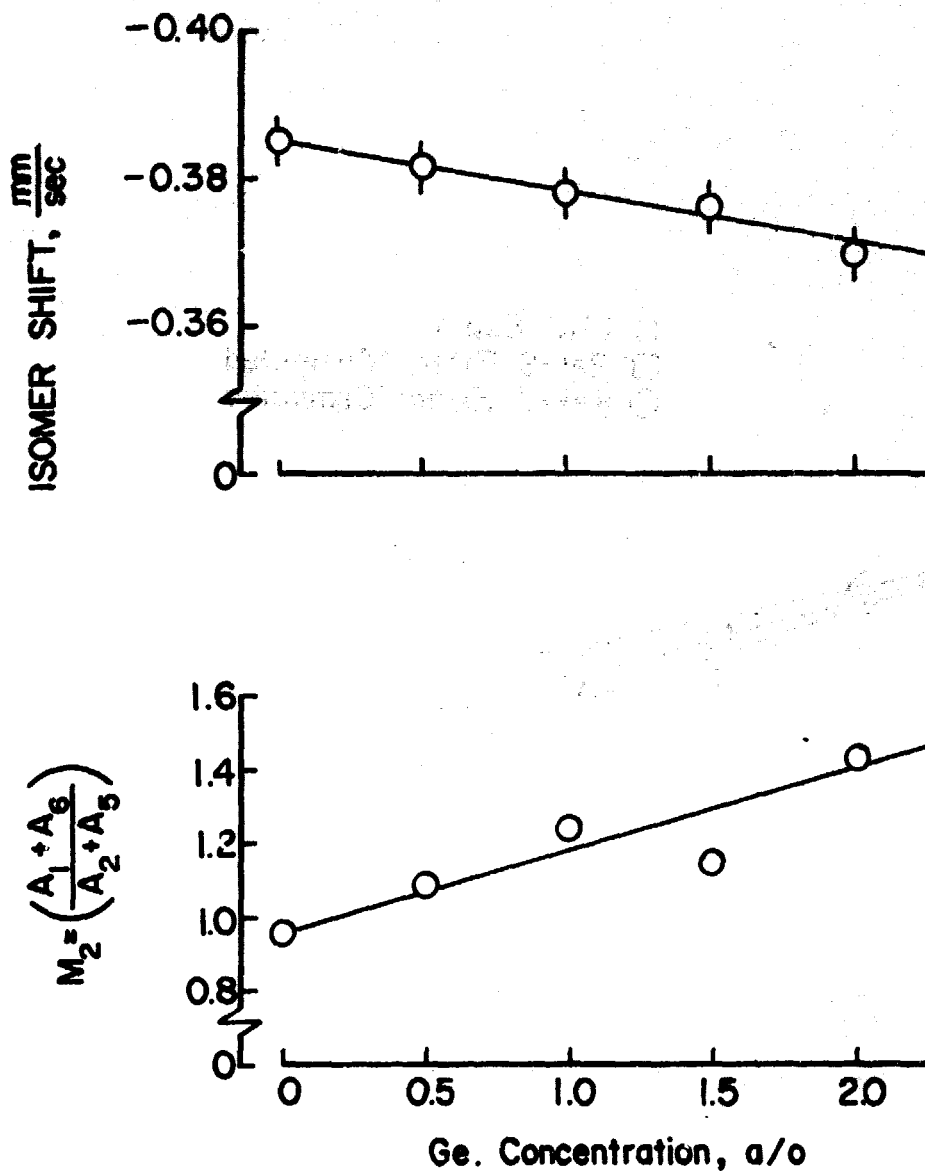


Figure - 6(b). Mossbauer parameter variation in (Fe-Ge) alloy as a function of Ge Concentration.

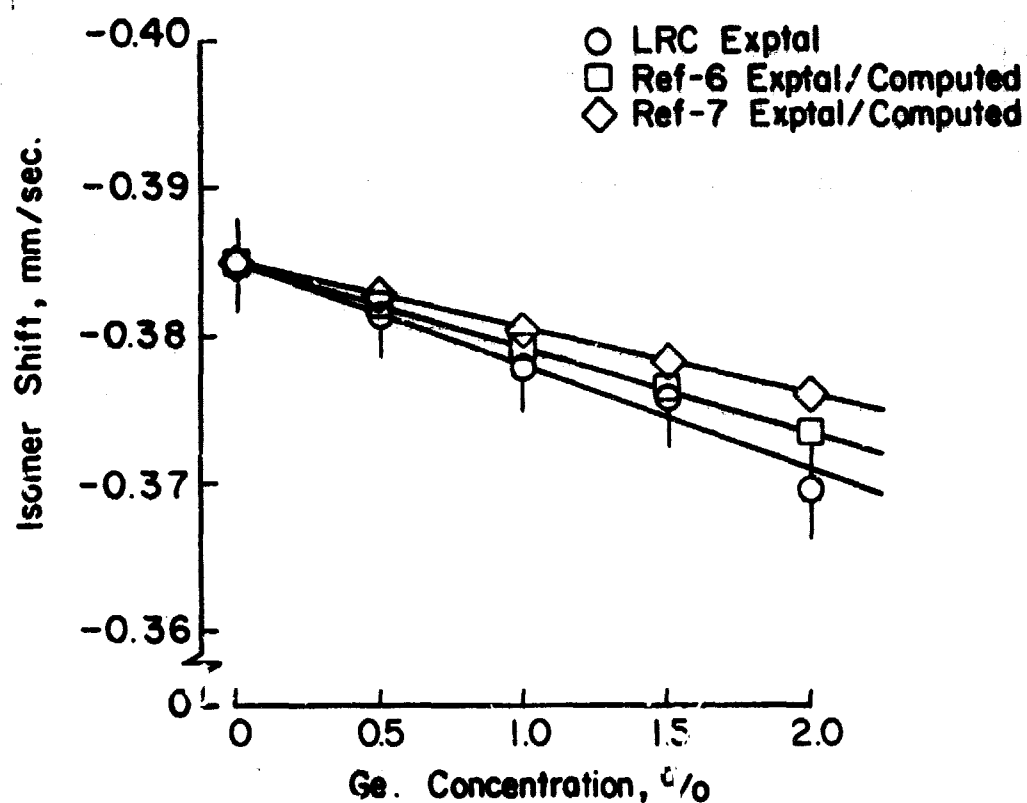


Figure-6(c). Isomer Shift variation in (Fe-Ge) alloy as a function of Ge Concentration. Also shown are data for (Fe-Si) alloy from Refs 6 and 7.

- Experimental Data for (Fe-Ge)
- Computed (Ref. 6 and 7) for (Fe-Si)
- ◇ Computed (Ref. 6) for (Fe-Sn)

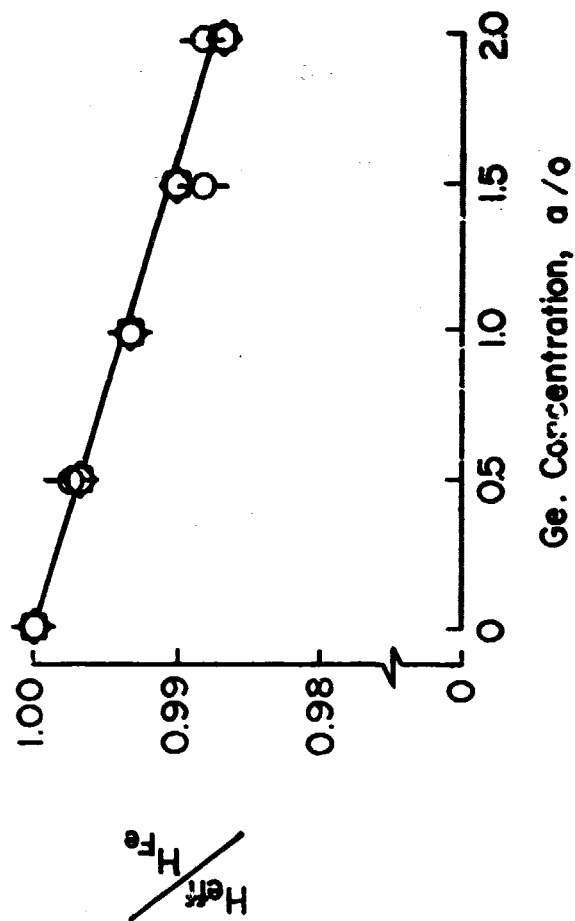


Figure - 7. Reduction in hfs field as a function of Ge Concentration in (Fe-Ge) alloy.

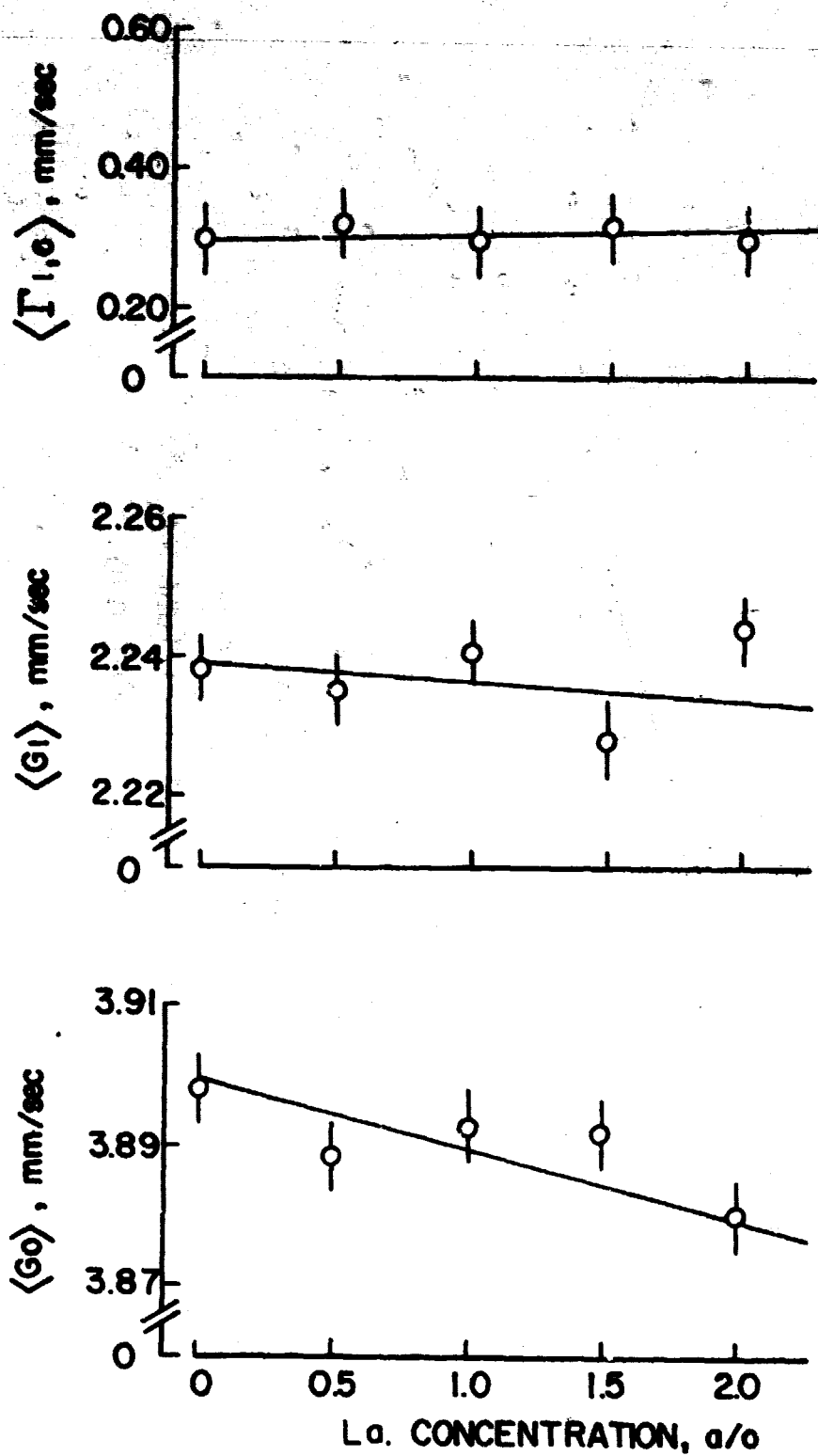


FIGURE-8(a). MOSSBAUER PARAMETER VARIATION IN (Fe-LA) ALLOY AS A FUNCTION OF LA CONCENTRATION.

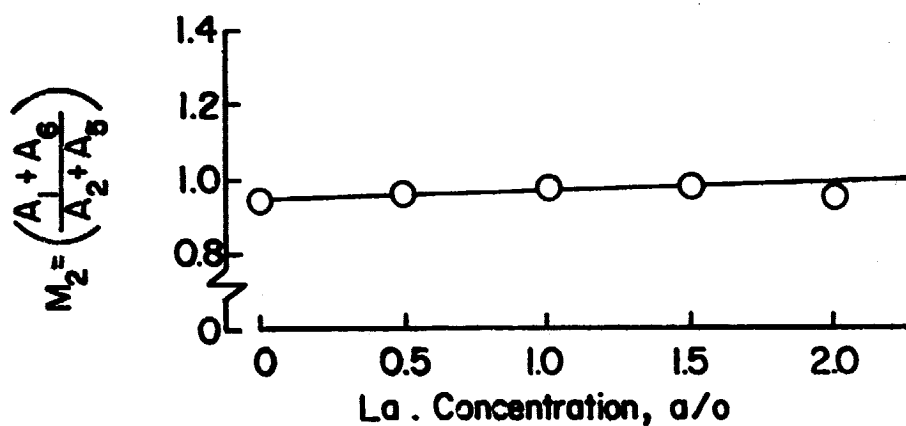
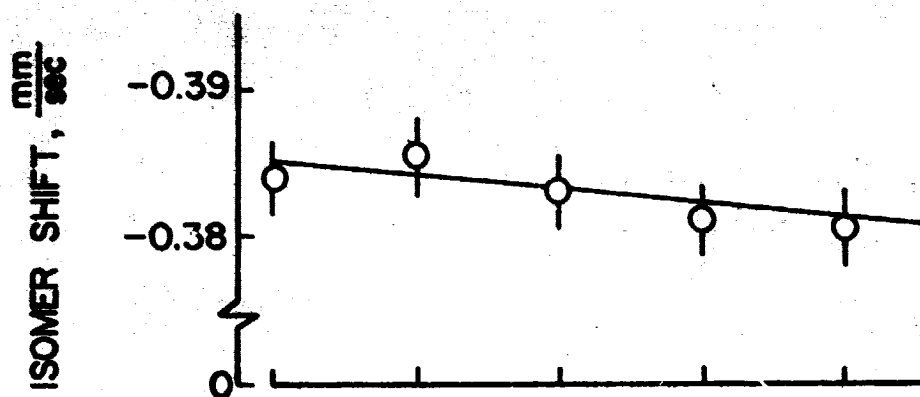


Figure - 8 (b). Mossbauer parameter variation in (Fe-La) alloy as a function of La Concentration.

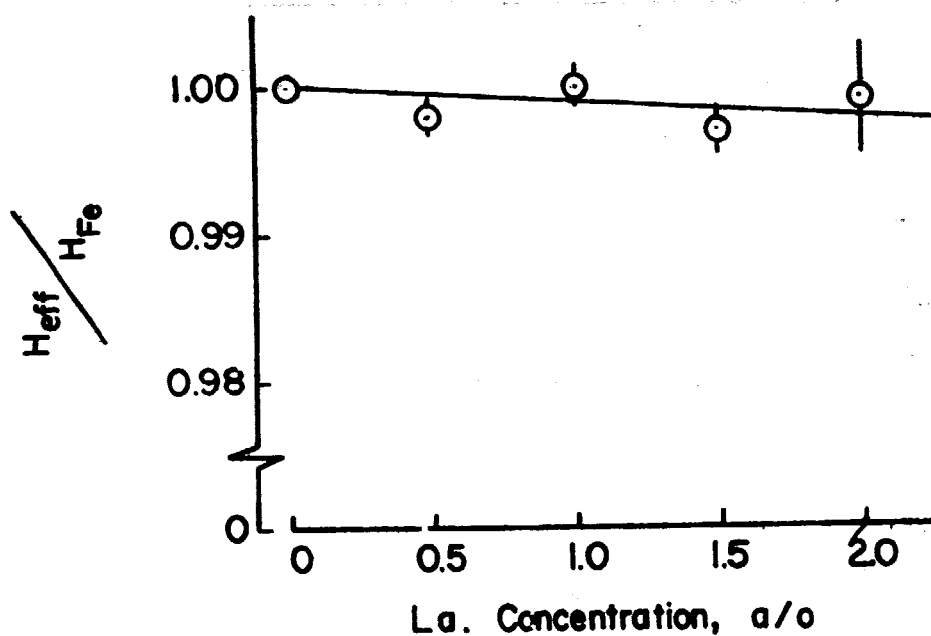


Figure-9. Reduction in hfs field as a function of La Concentration in (Fe-La) alloy.

APPENDIX A

APPROXIMATE FIT OF UNRESOLVED MOSSBAUER SPECTRA

WITH A SINGLE LORENTZIAN LINE

It is often necessary to fit an unresolved experimental spectrum, $I(x)$, with a single Lorentzian line if sufficient information is not available to permit a detailed resolution into its constituent spectra, $I(x)_i$. The compound line parameters (intensity I , peak position A , and peak width Γ) are related to the moments of distribution, as seen below:

$$\begin{aligned}
 I(x) &= \sum_i I(x)_i \\
 &= I_0 \sum_{i=1}^n \frac{\omega_i}{(x - a_i)^2 + \Gamma_0^2/4} \\
 &= I_0 \sum_{i=1}^n \frac{\omega_i}{\left[\Gamma_0^2/4 (x - a_i)^2/\Gamma_0^2/4 + 1 \right]}
 \end{aligned} \tag{1}$$

where ω_i = relative intensity of the i th component

a_i = peak position of the i th component

Γ_0 = component line width (assumed equal for all components)

and

$$\sum_i \omega_i = 1 \tag{2}$$

For data analysis, we minimize the following integral: ⁽⁸⁾

$$\int_{-\alpha}^{\alpha} \left(I_0 \sum_{i=1}^n \frac{\omega_i}{(x - a_i)^2 + \Gamma_0^2/4} - \frac{I}{(x - A)^2 + \Gamma^2/4} \right)^2 dx \tag{3}$$

Differentiating (3) with respect to I , A , and Γ and integrating over x leads to the following equations:

$$\left. \begin{aligned} \sum_{i=1}^n \frac{\omega_i}{\left[4 \frac{(A - a_i)^2}{(\Gamma + \Gamma_0)^2} + 1 \right]} &= \frac{I (\Gamma + \Gamma_0)}{2 \Gamma_0 \Gamma} \\ \sum_{i=1}^n \frac{\omega_i (A - a_i)}{\left[4 \frac{(A - a_i)^2}{(\Gamma + \Gamma_0)^2} + 1 \right]^2} &= 0 \\ \sum_{i=1}^n \frac{\omega_i (A - a_i)}{\left[4 \frac{(A - a_i)^2}{(\Gamma + \Gamma_0)^2} + 1 \right]^2} &= \frac{I (\Gamma + \Gamma_0)^2 (\Gamma^2 - \Gamma_0^2)}{32 \Gamma_0 \Gamma \Gamma_0} \end{aligned} \right\} \quad (4)$$

In case $|A - a_i| < \left(\frac{\Gamma + \Gamma_0}{2} \right)$, we can expand the denominators of the terms on the left hand side in equation (4) with the introduction of the following moments.

$$\left. \begin{aligned} \langle a \rangle &= \sum_{i=1}^n \omega_i a_i \\ M_2 &= \sum_{i=1}^n \omega_i (a_i - \langle a \rangle)^2 \end{aligned} \right\} \quad (5)$$

The final results are:

$$\left. \begin{aligned} \Gamma^2 &= \Gamma_0^2 + 8 M_2 - 8 \frac{2 M_4 - 3 M_2^2}{\Gamma^2} + \dots \\ A &= \langle a \rangle - 2 \frac{M_3}{\Gamma^2} + \frac{3 M_5 - 20 M_2 M_3}{\Gamma^4} - \dots \\ I &= I_0 \left(1 - 3 \frac{M_2}{\Gamma^2} + \frac{5 M_4 - 16 M_2^2}{\Gamma^4} - \dots \right) \end{aligned} \right\} \quad (6)$$

It should be emphasized that the above approach is justifiable only if the compound spectrum is unresolved, i.e., $|A - a_1| < \Gamma$. Any components for which this condition is not satisfied will be clearly separated from the other lines and should not be included in the single line fit.

APPENDIX B

LOCAL MAGNETIC FIELDS IN Fe X ALLOYS

The magnetic field at the iron atom (nucleus) is affected by the number and location of the impurity atoms alloyed with iron. In a random binary solution, the probability of an iron atom having a certain number of impurity neighbors in certain neighboring shells is calculated as follows:

$$\begin{aligned}
 P(n)_i &= \text{probability of } n \text{ impurity atoms in } i\text{th nearest neighbor shell} \\
 &= \binom{N}{n} C^n (1 - C)^{N-n} \\
 &= \frac{N!}{n! (N - n)!} C^n (1 - C)^{N-n} \quad (1)
 \end{aligned}$$

where N = number of iron atoms in the i th shell in pure iron. (In bcc iron lattice, the number of atoms in the first through fifth shells are, respectively, 8, 6, 12, 24, and 8.)

C = impurity atomic fraction

The joint probability of n , m , o , p , and q impurity atoms in the first, second, third, fourth, and fifth shells, respectively, is given by:

$$P(n, m, o, p, q) = P_1(n) P_2(m) P_3(o) P_4(p) P_5(q) \quad (2)$$

Using equation (2), we calculate below the probabilities for various combinations of impurity atoms in the two innermost shells, for two different levels of impurity atom concentration.

Coordination Combination Probability	Impurity Concentration 0.5 a/o	Impurity Concentration 2.0 a/o
P (0, 0)	0.9321	0.7536
P (0, 1)	0.0375	0.1230
P (1, 0)	0.0281	0.0923
P (1, 1)	0.0011	0.0151
P (0, 2)	0.0040	0.0047
P (2, 0)	0.0007	0.0088
P (2, 1)	0.000021	0.00107
P (1, 2)	0.000015	0.00080
P (3, 0)	0.000007	0.00035
P (0, 3)	0.000003	0.00013
ΣP_i	0.99995	0.99985

Thus for impurity concentrations < 2.0 a/o in Fe X alloys, there is an extremely small chance of simultaneously having more than three impurity atoms in the two innermost coordination shells. Actually, the probability of simultaneously having more than two impurity atoms in the two innermost shells is only 0.0025 even at 2.0 a/o.

The effects of impurity atoms in the two innermost coordination shells can be approximated by the following equation.

$$H(n, m) = H_0 (1 + an + bm) (1 + kc, \quad (3)$$

when H_0 = pure iron field a and b represent the fractional changes in hfs field per 1 nn and 2 nn impurity atoms, respectively. The concentration dependent factor k may contain unresolved effects of more distant neighbors. Introducing the effects of relative probability for various (n, m) combinations of impurity atoms, the effective internal field in Fe X alloys can be calculated as follows:

$$H_{eff} = \sum_i P(n, m)_i [H(n, m)]_i / \sum_i P(n, m)_i \quad (4)$$

It should be mentioned that H_{eff} , as given by equation (4), has significance only when one can approximate the observed unresolved Mossbauer spectrum with a single Lorentzian line (see appendix A).